

This article appeared in a journal published by Elsevier. The attached copy is furnished to the author for internal non-commercial research and education use, including for instruction at the authors institution and sharing with colleagues.

Other uses, including reproduction and distribution, or selling or licensing copies, or posting to personal, institutional or third party websites are prohibited.

In most cases authors are permitted to post their version of the article (e.g. in Word or Tex form) to their personal website or institutional repository. Authors requiring further information regarding Elsevier's archiving and manuscript policies are encouraged to visit:

<http://www.elsevier.com/copyright>



Contents lists available at ScienceDirect

# Nuclear Instruments and Methods in Physics Research A

journal homepage: [www.elsevier.com/locate/nima](http://www.elsevier.com/locate/nima)

## Novel nanocrystalline Gd<sub>2</sub>O<sub>3</sub>(Eu) scintillator screens with a micro-pixel structure for high spatial resolution X-ray imaging

Bo Kyung Cha<sup>a,\*</sup>, Seung Jun Lee<sup>b</sup>, P. Muralidharan<sup>b</sup>, Do Kyung Kim<sup>b</sup>, Jong Yul Kim<sup>c</sup>, Gyuseong Cho<sup>c</sup>, Sungchae Jeon<sup>a</sup>, Young Huh<sup>a</sup>

<sup>a</sup> Advanced Medical Device Research Center, Korea Electrotechnology Research Institute, Gyeonggi-do, Republic of Korea

<sup>b</sup> Department of Materials Science and Engineering, Korea Advanced Institute of Science and Technology, Daejeon, Republic of Korea

<sup>c</sup> Department of Nuclear and Quantum Engineering, Korea Advanced Institute of Science and Technology, Daejeon, Republic of Korea

### ARTICLE INFO

Available online 13 January 2011

#### Keywords:

Pixelated scintillator  
Nanocrystalline Gd<sub>2</sub>O<sub>3</sub>:Eu scintillator  
Spatial resolution  
X-ray imaging detector

### ABSTRACT

We developed a novel pixel-structured scintillation screen with nanocrystalline Gd<sub>2</sub>O<sub>3</sub>:Eu particle sizes for high spatial resolution X-ray imaging detectors. Nanocrystalline Gd<sub>2</sub>O<sub>3</sub>:Eu scintillators were successfully synthesized with a hydrothermal method and a subsequent calcination treatment, which were used as a material for converting incident X-rays into visible light. In this work, silicon-based pixel structures with different 100, 50 and 30 μm pixel sizes, a 10 μm wall width and a 120 μm thickness were prepared with the standard photolithography and the deep reactive ion etching (DRIE) process. Subsequently, a micro-pixel-structured scintillation screen was fabricated by adding the synthesized nanocrystalline Gd<sub>2</sub>O<sub>3</sub>:Eu scintillating phosphor to pixel-structured silicon arrays. Additionally, X-ray imaging performance such as relative light intensity, X-ray to light response and the spatial resolution in terms of modulation transfer function (MTF) were measured by using an X-ray source and a lens-coupled charge coupled device (CCD) camera system. The light intensity of the pixel-structured nanocrystalline Gd<sub>2</sub>O<sub>3</sub>:Eu screen was much higher than that of a pixel-structured sample made with a commercial microcrystalline Gd<sub>2</sub>O<sub>3</sub>:Eu product due to the density of the nanocrystalline Gd<sub>2</sub>O<sub>3</sub>:Eu scintillating powder-filled silicon structure. As the pixel size of the pixel-structured silicon decreased, the light intensity decreased. However, as the pixel size decreased, the spatial resolution significantly improved with no evident crosstalk from the emitted optical photons between adjacent scintillating pixels. The MTF of pixel-structured nanocrystalline Gd<sub>2</sub>O<sub>3</sub>:Eu screens with a 100 and a 50 μm pixel size was 20% and 30% at 6 lp/mm, respectively. As a result, this new technology showed that a microchannel structure based on a nanocrystalline Gd<sub>2</sub>O<sub>3</sub>:Eu scintillator could provide higher light intensity and high spatial resolution imaging compared to conventional microcrystalline scintillating phosphor.

© 2011 Elsevier B.V. All rights reserved.

### 1. Introduction

Indirect detection methods for digital X-ray imaging requires a scintillator film (a material that converts X-rays to visible light) and a 2D imaging sensor such as a-Si:H flat panel, CCD or CMOS imaging devices. The spatial resolution of an indirect X-ray imaging detector, unlike direct X-ray conversion methods, is currently limited by a lateral spreading effect (or crosstalk) of emitted light that depends on the thickness of the used scintillating layer [1]. Higher spatial resolution X-ray imaging is needed for medical diagnostic applications such as mammography, dental imaging and micro-CTs (computed tomography). An alternative solution for solving the spreading effect problem is to use pixelated scintillation films with polymer or silicon based-pixel structure arrays in order to prevent crosstalk between optical photons to individual neighboring pixels [2,3]. In this study, pixel-structured silicon arrays were used as light guides

and filled with advanced nanocrystalline scintillator instead of conventional microcrystalline scintillating phosphor to obtain a higher packing density [4]. Our new nanocrystalline europium-doped gadolinium oxide (Gd<sub>2</sub>O<sub>3</sub>:Eu) scintillating phosphor was fabricated through hydrothermal synthesis. Using a pixel-structured silicon array with different pixel sizes fabricated through the DRIE process on a silicon wafer, we prepared pixel-structured screens in various sizes with nanocrystalline Gd<sub>2</sub>O<sub>3</sub>:Eu scintillating phosphor. Additionally, we tested X-ray imaging performance, including relative light intensity, X-ray to light response, spatial resolution in terms of modulation transfer function (MTF), and object phantom of fabricated samples.

### 2. Materials and methods

Nanocrystalline Gd<sub>2</sub>O<sub>3</sub>:Eu scintillating powders with an average particle size of 100 nm were synthesized by a hydrothermal process. And a synthesized sample with an optimal calcination

\* Corresponding author.

E-mail addresses: [goldrain99@gmail.com](mailto:goldrain99@gmail.com), [goldrain99@kaist.ac.kr](mailto:goldrain99@kaist.ac.kr) (B.K. Cha).

temperature and time was heat-treated in an electric furnace in order to obtain the nanocrystalline  $Gd_2O_3:Eu$  scintillating powders, which had high light output under incident X-ray exposure [5,7]. Powdered- $Gd_2O_3:Eu$  scintillating screens were manufactured with a  $120\ \mu m$  thickness with a particle in binder (PIB) method and screen printing (SP). The detailed fabrication procedures of paste-typed  $Gd_2O_3:Eu$  solution were previously described in Ref. [6]. The pixel-structured nanocrystalline  $Gd_2O_3:Eu$  scintillating screens were fabricated by filling the fabricated paste, including nano-sized  $Gd_2O_3:Eu$  powders, into pixel-structured silicon array molds with 100, 50 and  $30\ \mu m$  pixel sizes with a vacuum process [2,6].

The microstructures of nanocrystalline  $Gd_2O_3:Eu$  scintillating screens with or without pixel-structured silicon arrays were investigated with FE-SEM (JEM-2100F HR). X-ray imaging performance parameters, such as relative light output, the light response to X-ray exposure dose and spatial resolution, were measured. A lens-coupled CCD imaging device with a  $1024 \times 1024$  pixel and an effective  $39\ \mu m$  pixel size (Andor DV-434) was used as a readout pixel array for visible photons emitted from the fabricated  $Gd_2O_3:Eu$  scintillating screens in an experimental X-ray radiographic system [6].

### 3. Results and discussion

An optical image of the pixelated  $Gd_2O_3:Eu$  scintillation screen with a  $2.5 \times 2.5\ cm^2$  size and SEM images of pixel-structured silicon arrays with 100 and  $50\ \mu m$  pixel sizes, a  $120\ \mu m$  pore depth generated by photolithography and deep reactive ion etching (DRIE)

process are shown in Fig. 1. Cross-section and surface images of nanocrystalline  $Gd_2O_3:Eu$  scintillating screens filled with pixel-structured silicon arrays for the 100 and  $50\ \mu m$  pixel sizes are shown in Fig. 2. Also, the cross-section and top views of the pixel-structured silicon array molds filled with commercial  $Gd_2O_3:Eu$  scintillator (Phosphor Technology, UK), which had an average particle size of  $5\ \mu m$  are shown in Fig. 3. From both Figs. 2 and 3 SEM images, the micro-pixel-structured  $Gd_2O_3:Eu$  scintillating screens using the nano-sized powders fabricated through a hydrothermal synthesis showed better uniformity and higher packing density with fewer voids compared to the commercial  $Gd_2O_3:Eu$ .

The relative light output from the fabricated  $Gd_2O_3:Eu$  scintillation screens was measured by the average pixel value of a region of interest (ROI) from X-ray images acquired under 50 kVp, 30 mAs X-ray exposure conditions. As the pore size of the pixel-structured silicon array decreased, the light output of the nanocrystalline and microcrystalline  $Gd_2O_3:Eu$  scintillating screens was reduced significantly. This trend is evident in Fig. 4. However, the light output of the pixel-structured  $Gd_2O_3:Eu$  scintillation screen with synthesized nanocrystalline powders was higher than the light output for commercial micro-sized particles since the nanocrystalline  $Gd_2O_3:Eu$  scintillator fabricated with a hydrothermal process showed light intensity that was 1.5 times higher than the commercial product (Fig. 4). There were also fewer voids and more densely packed filling of nanocrystalline scintillating particles in the pixel-structured silicon array (see Figs. 2 and 3). However, the relative light intensity of pixel-structured  $Gd_2O_3:Eu$  screens with both commercial microcrystalline particles and nanocrystalline particles was much lower than the light intensity of non-pixel structured (or continuous)  $Gd_2O_3:Eu$  screens since

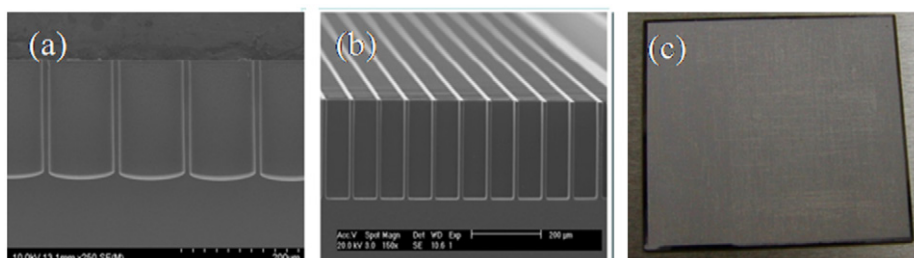


Fig. 1. SEM images of pixel-structured silicon arrays with (a) 100 and (b)  $50\ \mu m$  pixel size. (c) A picture of pixel-structured  $Gd_2O_3:Eu$  scintillating screen.

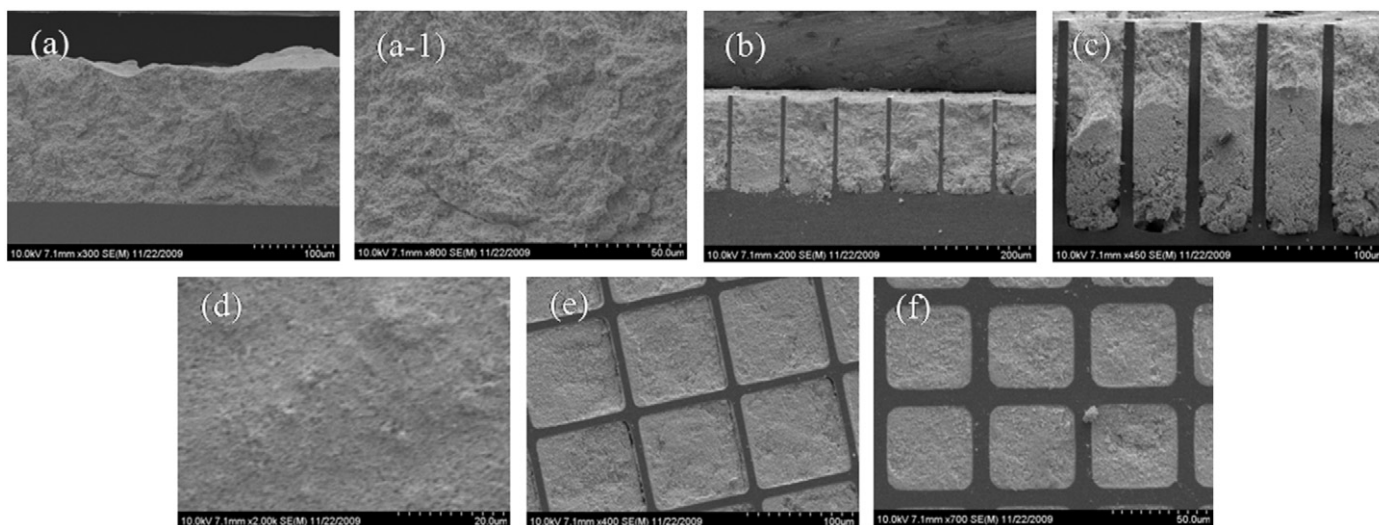
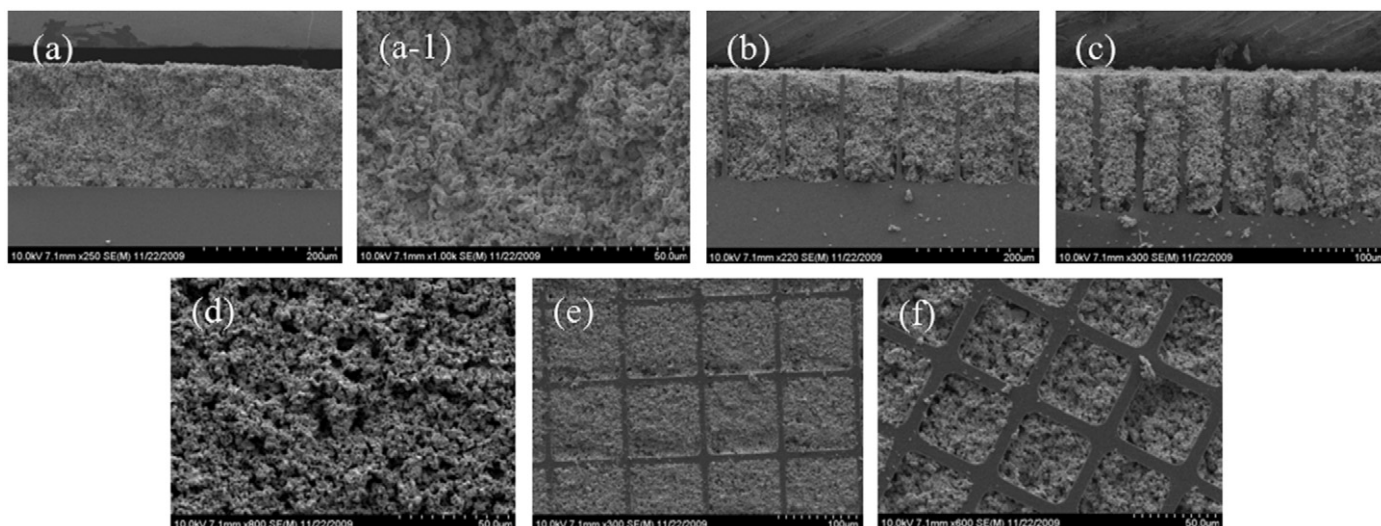
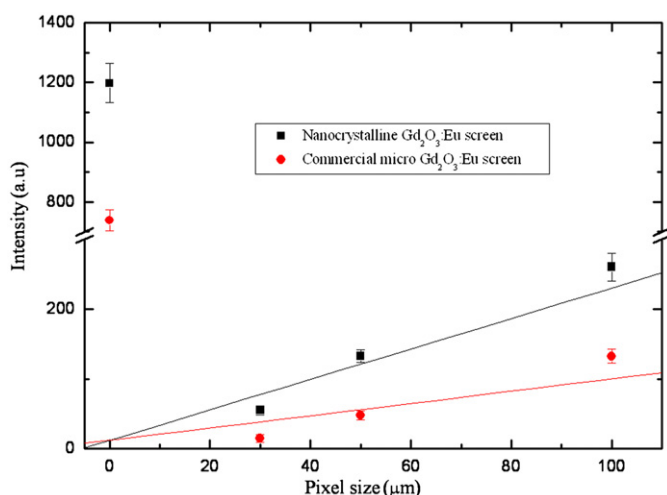


Fig. 2. SEM images of pixel-structured nanocrystalline  $Gd_2O_3:Eu$  scintillating screen layer. Cross-section of (a) non-pixel, (a-1) enlarged non-pixel, (b) 100 and (c)  $50\ \mu m$  pixel size. Surface section of (d) non-pixel, (e) 100 and (f)  $50\ \mu m$  pixel size.



**Fig. 3.** SEM images of pixel-structured commercial  $Gd_2O_3:Eu$  scintillating screen layer. Cross-section of (a) non-pixel, (a-1) enlarged non-pixel, (b) 100 and (c) 50  $\mu m$  pixel size. Surface section of (d) non-pixel, (e) 100 and (f) 50  $\mu m$  pixel size.



**Fig. 4.** Light intensity of commercial micro- and nano-crystalline  $Gd_2O_3:Eu$  screens as a function of pixel size.

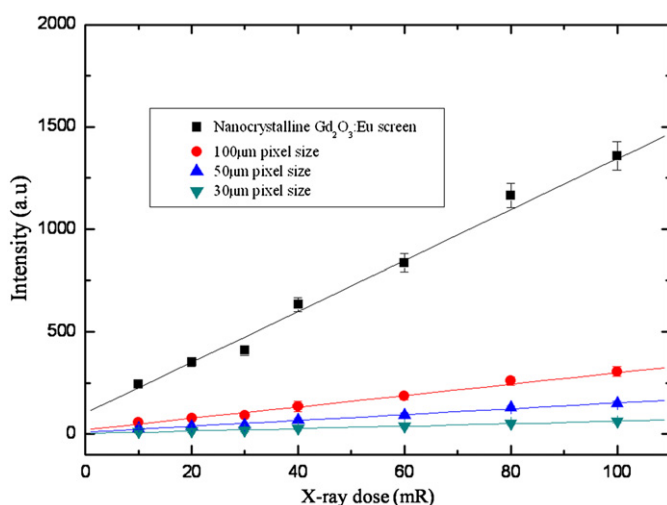


**Fig. 5.** X-ray linearity of nanocrystalline  $Gd_2O_3:Eu$  screens with different pixel sizes as a function of X-ray exposure dose.

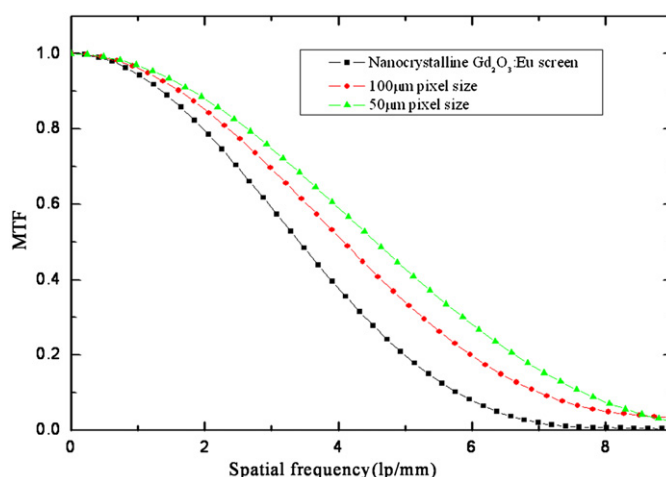


**Fig. 6.** Spatial resolution of nanocrystalline  $Gd_2O_3:Eu$  screens with different pixel sizes.

the visible photons generated within the scintillating layers were scattered and absorbed in the silicon wall surfaces [8,9]. The light intensities of pixel-structured samples with 30, 50 and 100  $\mu m$  pixel sizes were approximately 5%, 11% and 22%, respectively, compared to the continuous 150  $\mu m$ -thick nanocrystalline  $Gd_2O_3:Eu$  scintillating screens.

The X-ray to light response of nanocrystalline  $Gd_2O_3:Eu$  scintillating screens with different pixel sizes was measured as a function of X-ray dose and the measured results were plotted in Fig. 5. As the X-ray exposure dose increased, light output of all the fabricated nanocrystalline  $Gd_2O_3:Eu$  scintillation screens with and without a pixel-structured silicon array showed a linear increase. The MTF results are plotted in terms of spatial resolution in Fig. 6 and the X-ray images obtained with a memory chip phantom are displayed in Fig. 7. The spatial resolution of non-pixel-structured and pixel-structured nanocrystalline  $Gd_2O_3:Eu$  scintillating screens with 100 and 50  $\mu m$  pixel sizes had 10%, 20% and 30% MTF values at a spatial frequency of 6 lp/mm. Sharper X-ray images were obtained by using nanocrystalline  $Gd_2O_3:Eu$  scintillating screens with micro-pixel-structured silicon arrays, which are shown in Fig. 7. It was expected that the spatial resolution would largely be enhanced by a pixel-structured scintillating

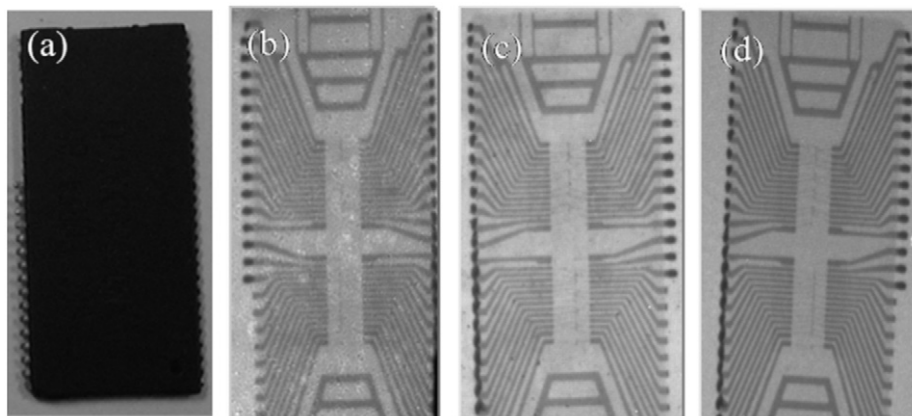


Fig. 7. X-ray images of nanocrystalline  $\text{Gd}_2\text{O}_3:\text{Eu}$  screens with different pixel sizes. (a) A memory chip, (b) non-pixel, (c) 100 and (d) 50  $\mu\text{m}$  pixel size.

screen with a smaller pixel size. However, because smaller pixel size in pixel-structured nanocrystalline  $\text{Gd}_2\text{O}_3:\text{Eu}$  screens was used to improve spatial resolution, there was a significant decrease in the light intensity. As such, additional research to enhance the spatial resolution of X-ray imaging without sacrificing light intensity is needed.

#### 4. Conclusion

Novel micro-pixel structured screens with nanocrystalline  $\text{Gd}_2\text{O}_3:\text{Eu}$  scintillating phosphor were fabricated and the X-ray imaging parameters, such as relative light output, X-ray linearity and spatial resolution were characterized. In this study, the nanocrystalline  $\text{Gd}_2\text{O}_3:\text{Eu}$  scintillator fabricated through a hydrothermal process instead of a commercial microcrystalline  $\text{Gd}_2\text{O}_3:\text{Eu}$  scintillator was utilized to increase the light intensity and the packing density of the pixel-structured scintillating screens while maintaining a high spatial resolution. However, substantial effort is still required to improve the light guiding efficiency of pixel-structured scintillation screens while maintaining high spatial resolution for X-ray imaging.

#### Acknowledgements

This research was supported by the Korea Electrotechnology Research Institute (KERI) and funded by the Ministry of Knowledge Economy (10-12-N0201-09).

#### References

- [1] Luís Lança, Augusto Silva, *Radiography* 15 (2009) 58.
- [2] S. Tao, Z.H. Gu, A. Nathan, *J. Vac. Sci. Technol. A* 20 (3) (2002) 1091.
- [3] Olof Svenonius, Anna Sahlholm, Per Wiklund, Jan Linnros, *Nucl. Instr. and Meth. A* 607 (2009) 138.
- [4] Muralidhar Mupparapu, Rameshwar N. Bhargava, Satish Mullick, Steven R. Singer, Nikhil Taskar, Aleksey Yekimov, *Int. Cong. Ser.* 1281 (2005) 1256.
- [5] P. Muralidhran, Seung Jun Lee, Bo Kyung Cha, Joung Yul Kim, Chan Kyu Kim, Do Kyung Kim, Gyuseong Cho, in: *Proceedings of the IEEE Nuclear Science Symposium Conference Record, NS25 (108)*, 2009, pp. 1486.
- [6] Bo Kyung Cha, Jong Yul Kim, Tae Joo Kim, Cheulmuu Sim, Gyuseong Cho, *Radiat. Meas.* 45 (2010) 742.
- [7] Ying Tian, Wang-He Cao, Xi-Xian Luo, Yao Fu, *J. Alloys Compd.* 433 (2007) 313.
- [8] X. Badel, A. Galeckas, J. Linnros, P. Kleimann, C. Fröjd, C.S. Petersson, *Nucl. Instr. and Meth. A* 487 (2002) 129.
- [9] Matthias Simon, Klaus Jürgen Engel, Bernd Menser, Xavier Badel, Jan Linnros, *Med. Phys.* 35 (3) (2008) 968.